AGU PUBLICATIONS

Geophysical Research Letters

RESEARCH LETTER
10.1002/2017GL076250

Key Points:
- Change in ENSO variability during the last 6,000 years is mainly induced by an orbital forcing only without invoking other climate forcing
- The zonal and meridional gradients of mean tropical SST were gradually reduced during the last 6,000 years ago
- The horizontal thermal advections associated with mean SST gradient are critical in modifying ENSO activity for the last 6,000 years

Correspondence to:
S.-I. An,
sian@yonsei.ac.kr

Citation:
An, S.-I., Im, S.-H., & Jun, S.-Y. (2018). Changes in ENSO activity during the last 6,000 years modulated by background climate state. *Geophysical Research Letters*, *45*. https://doi.org/10.1002/2017GL076250

Received 31 OCT 2017
Accepted 22 FEB 2018
Accepted article online 28 FEB 2018

Changes in ENSO Activity During the Last 6,000 Years Modulated by Background Climate State

Soon-Il An[1], Seul-Hee Im[1], and Sang-Yoon Jun[2]

[1]Department of Atmospheric Sciences, Yonsei University, Seoul, South Korea, [2]Korea Polar Research Institute, Incheon, South Korea

Abstract Various proxy records show that El Niño–Southern Oscillation (ENSO) activity has changed from calm to active during the last 6,000 years. However, it is so far unclear whether orbital forcing has solely induced such a dramatic change. In this study, we performed a transient run for the last 6,000 years using an Earth system model of intermediate complexity affected by orbital forcing only without changes due to other climate forcing, and then its time-varying background states were implemented into an intermediate atmosphere-ocean coupled model for ENSO. ENSO activity simulated by the intermediate atmosphere-ocean coupled model during the last 6,000 years resembled the observed proxy data, inferring that orbital forcing mainly leads to changes in ENSO activity during the last 6,000 years. From additional sensitivity experiments, we found that a change in sea surface temperature background conditions is primarily responsible for the observed ENSO activity over the last 6,000 years through modifying the anomalous horizontal thermal advection of the mean SST gradient.

1. Introduction

The El Niño–Southern Oscillation (ENSO) is one of the most distinct climate phenomena and occurs quasiperiodically over the tropical Pacific. Although it arises due to a large-scale atmosphere-ocean interaction (Bjerknes, 1966), its impact reaches all over the globe (McPhaden et al., 2006). Since the growth of ENSO is attributed to the air-sea coupled feedback, a change in air-sea coupled stability obviously modifies the characteristics of ENSO. In particular, coupled stability depends on mean state conditions (e.g., An & Bong, 2016; An & Jin, 2000; An & Wang, 2000), and thus, a long-term change in these has likely influenced the ENSO (e.g., An & Jin, 2000; Liu et al., 2014; Wang & An, 2001).

When exactly the strong modern ENSO began to appear in the Holocene era is not clearly known. So far, many studies based on proxy data have claimed that the modern ENSO started during the late Holocene (about 2 to 3,000 years before present [B.P.]), and various paleoclimate records including corals, archeological middens, and lake and ocean sediments have revealed that ENSO activity during the early to mid-Holocene (MH) was weak (McGregor & Gagan, 2004; Moy et al., 2002; Tudhope et al., 2001). Finally, ENSO activity since the early Holocene has been gradually increasing (Conroy et al., 2008; Koutavas & Joanides, 2012; Moy et al., 2002; Rein et al., 2005). Since ENSO characteristics, particularly its activity, depend on the mean climate state, it is worth understanding how this has changed during the Holocene era, particularly during the last 6,000 years, which is the time period of our target to evaluate ENSO activity. Actually, from 6,000 years B.P. to the preindustrial (PI) era, major climate forcing such as greenhouse gas concentration and geographical configuration including continental ice sheets have not significantly changed except for orbital forcing, and so the major difference in the climate forcing used in the time-slice simulations at 6,000 years B.P. of Paleoclimate Model Intercomparison Projects (PMIPs) compared to the PI simulation was the orbital forcing. Therefore, it is expected that a change in the mean state associated with a change in orbital forcing led to a change in ENSO activity (e.g., Clement et al., 1999, 2000; Liu et al., 2014).

In PMIPs, the time-slice simulations at 21,000 years B.P. (the Last Glacial Maximum simulation), 6,000 years B.P. (MH simulation), and the PI period (PI simulation) were performed. Some other coupled general circulation models that did not participate in PMIPs also simulated climate variability for fixed climate forcing. These experiments were not able to support a continuous picture to depict a gradual change in ENSO activity associated with a slow and gradual change in mean state. Recently, a transient experiment continuously running from 22,000 years B.P. to present has been performed using the Community Climate System Model Version 3, the so-called baseline transient simulation (TraCE; http://www.cgd.ucar.edu/ccr/TraCE/), in which the orbital,

greenhouse concentration, volcanic eruption, continental ice sheet topography, meltwater discharge into Atlantic Ocean, and costal change associated with sea level change were taken into account. Using TraCE output from this, Liu et al. (2014) analyzed changes in ENSO since the Last Glacial Maximum and concluded that its strengthening is attributed to orbital forcing via enhancing positive atmosphere-ocean feedback (especially Ekman feedback [local upwelling]). Their study provided a continuous feature in the changing of ENSO activity as well as answered the question on which climate forcing is responsible for the change in ENSO activity. In particular, they mentioned that the orbital forcing only experiment almost reproduced the slowly varying change in ENSO amplitude. However, the orbital forcing only experiment in TraCE did not show a significant increasing trend in ENSO amplitude during the last 6,000 years (Liu et al., 2014).

El Niño–Southern Oscillation variability can be modulated by the slow undulation of mean climate conditions via changing the stability of the tropical Pacific air-sea coupled system (An & Bong, 2018; An & Wang, 2000; Fedorov & Philander, 2001), altering a nonlinear process such as ENSO bursting in a particular nonlinear regime (Timmermann et al., 2003), varying nonlinear interaction with the annual cycle (Jin et al., 1994), and either additive or multiplicative stochastic forcing (Flügel & Chang, 1999; Flügel et al., 2004; Jin et al., 2007; Thompson & Battisti, 2001; Yeh & Kirtman, 2004). However, which of these can be mainly attributed to the change in ENSO activity during the last 6,000 years was not exactly addressed in Liu et al. (2014). Herein, we predominantly focus on the effect of the slow change in mean climate conditions on the change in ENSO activity. Therefore, we address the following questions: (1) Does the slow undulation of climate background state during the last 6,000 years associated with changes in orbital forcing solely produce ENSO variability to be similar to as observed? (2) Which variable of climate state is the most influential on modifying ENSO activity? (3) What is the physical mechanism behind it?

To address the above questions, we performed a transient simulation for the last 6,000 years using an Earth system model of intermediate complexity (the LOch-Vecode-Ecbilt-CLio-agIsm Model: LOVECLIM), and then its simulated time-varying background climate state was adopted into the intermediate tropical Pacific atmosphere-ocean coupled model (the Zebiak-Cane model; hereafter the ZC model). In section 2, the models and experimental design are described, and results and concluding remarks are presented in sections 3 and 4, respectively.

2. Models and Experimental Design

2.1. LOch-Vecode-Ecbilt-CLio-agIsm Model

LOch-Vecode-Ecbilt-CLio-agIsm Model is an Earth system model composed of five different models (Goosse et al., 2010), namely, a global quasi-geostrophic atmospheric model truncated at T21 (ECBILT) (Opsteegh et al., 1998), a free-surface ocean general circulation model coupled to a thermodynamic-dynamic sea ice model (CLIO) (Goosse & Fichefet, 1999), a terrestrial vegetation module (VECODE) (Brovkin et al., 1997), Antarctica and Greenland Ice-Sheet Model (AGISM) (Huybrechts, 2002), and a three-dimensional oceanic carbon cycle model (LOCH) (Mouchet & François, 1996).

2.2. The intermediate atmosphere-ocean coupled model (the ZC model)

The ZC model (Zebiak & Cane, 1987) is an anomalous nonlinear atmosphere-ocean coupled model with a spatial domain in the tropical Pacific in which the seasonally varying background states obtained from the observation are prescribed. The atmospheric component is a Gill-type steady state linear model capturing the first baroclinic mode responding to the latent heating at the midtroposphere (Gill, 1980), and latent heating is composed of surface evaporation and low-level moisture convergence. The ocean dynamic model is a 1.5-layer reduced gravity linear model where the gravity wave speed is fixed at 2.9 ms^{-1} and the thermodynamic part of the ocean model simulates sea surface temperature (SST) anomalies mainly driven by three-dimensional thermal advection and linear Newtonian thermal damping, thereby mimicking a comprehensive surface heat flux exchange between the ocean surface and the atmosphere. The ZC model poses good capability for El Niño prediction (e.g., Cane & Zebiak, 1987; Chen et al., 1998).

2.3. Experimental design

Time integration of LOVECLIM started from 6,000 B.P. and finished at the present. During the integration, orbital forcing changed over time, while all other climate forcing factors, which are the same as those during

the PI era, were unchanged. Therefore, the LOVECLIM-produced output is a combination of natural variability and orbital-forcing induced change during the last 6,000 years.

Because of the low spatial resolution and simplified physical process in LOVECLIM, it is not capable of producing ENSO. On the other hand, the ZC model is anomalous with prescribed climate background conditions and thus cannot simulate the mean state. Therefore, the climate background states simulated by LOVECLIM were adopted for the ZC model.

In order to remove short-period fluctuation, 101 year moving average was applied to the LOVECLIM-produced output, and then the last 101 year mean was subtracted from the whole 6,000 year simulation; thus, deviations for the last 101 years actually became zero. To avoid strong impact due to change in the background state of ZC model, the deviations as time-varying background state were added to the original background states of ZC model. Therefore, the system of ZC model in this study became

$$\frac{d\vec{X}}{dt} = F\left[\vec{X}_c(0) + \Delta\vec{X}_M(t_M), \vec{X}(t)\right] \tag{1}$$

where $\vec{X}(t)$ is the state vector for the physical variables, namely, two-dimensional surface winds, three-dimensional currents in the mixed layer, ocean dynamics height, and the SST; $\vec{X}_c(0)$ are the seasonally varying climatological mean values of the physical variables at the present (t = 0) used in the original ZC model; $\Delta\vec{X}_M(t_M)$ are the differences in the annual mean values of the physical variables between the 101 year moving average and the last 101 year mean of the 6,000 year simulation with LOVECLIM; and t_M is the time for changing the background state.

In this study, the perturbed mean state (i.e., $\Delta\vec{X}_M$) included the SST, thermocline depth, vertical temperature gradient at the ocean mixed layer, and surface wind stress. Before perturbing the mean state over time, we performed two perpetual experiments: one with the present mean state ("0 ka-ZC run") and the other with 6 ka mean state ("6 ka-ZC run"). In 6 ka-ZC run, $\Delta\vec{X}_M(t_M = 6,000 \text{ years B.P.})$ was used. The transient experiment with time-varying mean state refers to the "Tran-ZC run."

We performed 51 runs for each experiment, and thus, the ensemble mean was taken from 51 ensembles. Stochastic additive noise as surface zonal wind was applied during all integrations, and the initial conditions for each run were taken under the same condition.

In the ZC model, SST equation is as follows:

$$\frac{\partial T}{\partial t} = -u\frac{\partial \overline{T}}{\partial x} - (\overline{u}+u)\frac{\partial T}{\partial x} - v\frac{\partial \overline{T}}{\partial y} - (\overline{v}+v)\frac{\partial T}{\partial y} - \{M(\overline{w}+w) - M(\overline{w})\}\frac{\partial \overline{T}}{\partial z} - M(\overline{w}+w)\frac{\partial T}{\partial z} - \alpha T \tag{2}$$

where u, v, and w represent the horizontal surface currents and upwelling; T is the temperature; α is a comprehensive thermodynamical damping coefficient; and $M(x) = x$ for $x > 0$, else $M(x) = 0$. The overbar indicates the climatological mean or else anomalies.

3. Results

The slow change in ENSO activity during the last 6,000 years obtained from our experiment (see section 2) was mainly driven by orbital forcing. Actually, the transient run for the last 21,000 years by Liu et al. (2014) also showed the amplitude modulation of ENSO since the MH was mainly driven by orbital forcing, which showed significant change during the last 6,000 years over the tropical Pacific (Figure 1a). When comparing 6,000 years B.P. to the present, insolation during late winter was weaker by 25 Wm^{-2} and that during late summer was stronger by 25 Wm^{-2}. Such enhanced seasonal contrast in insolation, which gradually reduced afterward, modified the seasonal cycle over the tropical Pacific, resulting in a weaker annual cycle over the tropical eastern Pacific (EP) 6,000 years ago (An & Choi, 2014).

On the other hand, changes in the mean state showed a location-dependent feature (Figure 1b) by which the global-mean and western Pacific temperature decreased, while the EP surface temperature increased. The decreasing global-mean temperature during the last 6,000 years was attributed to decreasing solar radiation over the Northern Hemisphere associated with changes in precession. Furthermore, the cooling tendencies over both the western and the whole of the Pacific were also related to the reduced solar radiation.

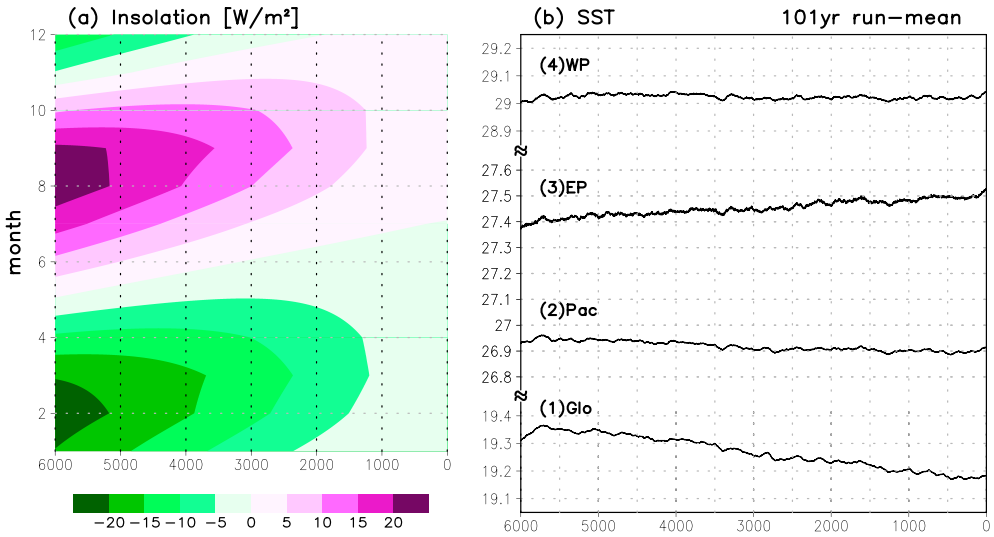

Figure 1. (a) Calculated deviation of the insolation from the present values at the top of the atmosphere over the equatorial region (5°S–5°N) during the last 6,000 years. (b) Simulated sea surface temperature averaged over the (1) global (0–360°, 80°S–80°N), (2) Pacific (100°E–70°W, 30°S–30°N), (3) eastern equatorial Pacific (150°W–90°W, 5°S–5°N), and (4) western equatorial Pacific (120°E–180°E, 5°S–5°N) areas. One hundred one-year moving average was applied to all of the time series in (b).

Conversely, the warming tendency over the EP was related to the dynamical response of cold tongue to the change in solar radiation. That is to say, the larger summer insolation over the Northern Hemisphere during the MH promoted the northward migration of the EP Intertropical Convergence Zone (ITCZ), which was accompanied by strong cross equatorial southerly winds over the equatorial EP, led to the cooling of the cold tongue via the enhanced equatorial upwelling. As the insolation on the Northern Hemisphere decreased, the ITCZ moved to the south, and consequently, the cold tongue temperature gradually increased. Therefore, the zonal SST contrast along the equatorial Pacific gradually decreased during the last 6,000 years. Interestingly, in both the observation and some coupled general circulation models, the zonal SST contrast between the equatorial western Pacific warm pool and the equatorial EP cold tongue is inversely proportional to ENSO variance (e.g., An & Choi, 2015; Koutavas & Joanides, 2012). Therefore, the decreasing tendency of the zonal contrast of equatorial Pacific SST may provide a clue as to why the ENSO activity gradually increased during the last 6,000 years.

So far, we have briefly discussed a possible mechanism on the impact of orbital forcing on ENSO activity via modifying the cold tongue temperature. To check the change in the spatial pattern of tropical Pacific climate state, we computed the difference in the ocean surface and subsurface climate condition between the last 100 years and the first 100 years obtained from the LOVECLIM 6,000 year simulation. The difference map basically represents the MH climate conditions with respect to their present state. As shown in Figure 2a, overall surface cooling over the equatorial Pacific with meridionally wider and cooler in the EP was observed, which was mainly due to the reduced mean insolation, and subtropical warming was also observed. Obviously, more cooling over the EP was related to the wind-induced upwelling cooling.

Associated with the SST pattern, the surface winds were southeasterly over the southern tropical Pacific up to 5°N and southwesterly over the northeastern tropical Pacific. Overall, a southerly wind led to the northward migration of the ITCZ, and the easterlies along the equator indicated an enhanced trade wind as well as equatorial upwelling during the MH. The oceanic response was also dynamically consistent to the enhanced trade wind, namely, the enhanced zonal slope of thermocline (Figure 2c). Furthermore, the vertical ocean temperature gradient measured at the mixed layer depth decreased, especially over the western-to-central Pacific (CP; Figure 2d). Obviously, these mean states influenced ENSO activity, which is discussed later.

Next, we show ENSO activity obtained from the ZC model in Figure 3. ENSO activity is depicted by the 101 year moving standard deviation (STD) of Niño-3 SST anomalies. The ENSO activity obtained from the 6 ka-ZC run was heavily suppressed (STD ~0) compared to that from the 0 ka-ZC run (STD ~1.1), and the two runs were completely separable (Figure 3a). It should be noted that ZC model is more capable for

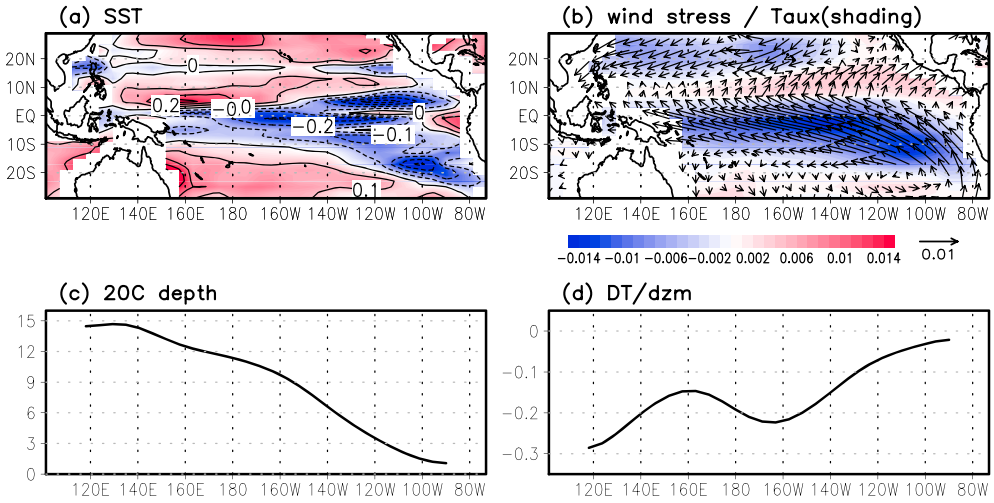

Figure 2. Difference between the past 100 year (6,000–5,900 B.P.) and recent 100 year (100–0 B.P.) mean values for (a) sea surface temperature, (b) surface wind stress, (c) 20°C isotherm depth along the equator, and (d) vertical temperature gradient along the equator. The shading in (b) indicates the difference in zonal wind stress. Twenty degrees Celsius isotherm depth and vertical temperature gradient were averaged over the equatorial band (5°S–5°N) and spatially smoothed. Positive isotherm depth means a deeper thermocline. Units are (a) °C, (b) N/m^2, (c) m, and (d) °C/100 m.

simulating EP-type El Niño than CP-type El Niño (e.g., Yeh et al., 2014), and thus, a strong suppression in 6 ka-ZC run infers to the suppression of EP El Niño but not CP El Niño, which is consistent with Karamperidou et al. (2015). As aforementioned, in the Tran-ZC run, four variables (SST, thermocline, vertical temperature gradient, and surface wind stress) were implemented into the background state of the ZC model (i.e., the control run). The ENSO amplitude fluctuations from the Tran-ZC run were as follows (red curve in

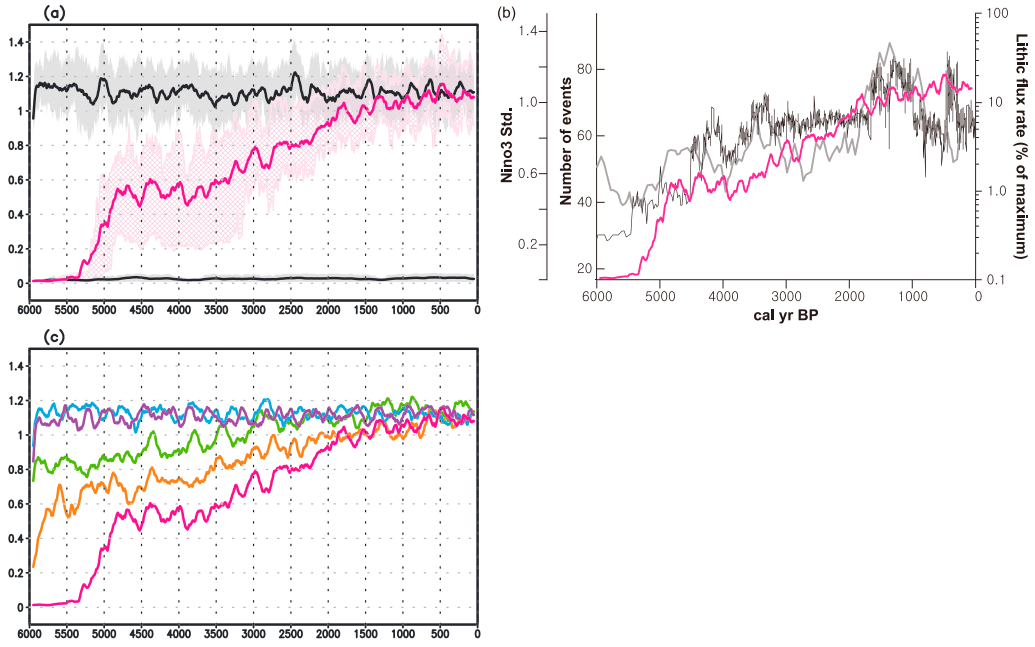

Figure 3. (a) One hundred one-year moving standard deviation of Niño3 sea surface temperature (SST) anomalies. The thick lines indicate the average of 51 ensembles, and the shaded areas specify the 25th–75th percentiles of the ensembles. The upper black, middle red, and lower black lines indicate the results from the present-condition experiment (0 ka-ZC run), the control experiment (Tran-ZC run), and the 6 ka experiment (6 ka-ZC run), respectively. (b) El Niño–Southern Oscillation activity during the last 6000 years: the lithic flux in marine sediments off Peru (black thin line; Rein et al., 2004, 2005) and the ZC-model results by Clement et al. (2000) (black thick line); the red line is the same line from the ensemble mean of (a). The black and gray lines were obtained from Figure 12 of Wanner et al. (2008). (c) One hundred one-year moving standard deviations of Niño3 SST anomalies obtained from ensemble mean of the SST_m (orange), H_m (green), $dTdz_m$ (blue), WS_m (purple), and control (red) experiments. Each line is the average of 51 ensembles: the same as in (a).

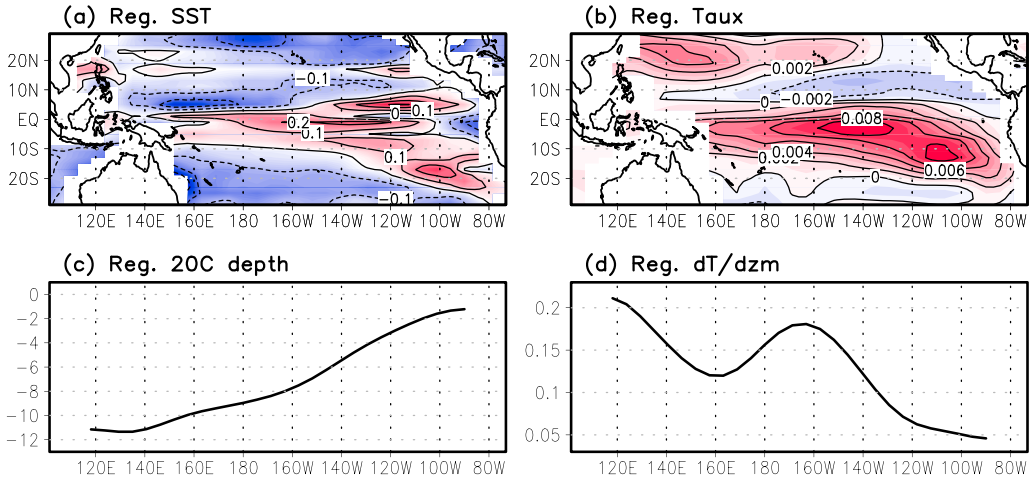

Figure 4. (a) Regression map of mean sea surface temperature (SST) against the 101 year moving standard deviation of the Niño-3 SST anomalies obtained from one ensemble member of the Tran-ZC runs. (b–d) As in (a) but for zonal wind stress, the equatorial-band (5°S–5°N) averaged 20°C isotherm depth, and the equatorial-band averaged vertical temperature gradient at a depth of 50 m.

Figure 3a): almost no fluctuation until 5,500 years B.P.; abrupt enhancement of ENSO amplitude occurred around 5,400 years B.P.; an increasing trend of ENSO amplitude during 3,300–4,700 years B.P.; the reappearance of a strong increasing trend in ENSO amplitude between 3,300 and 1,900 years B.P.; the very weak increasing trend of ENSO amplitude after 1,900 years B.P.; and finally, merging with the 0 ka-ZC run.

To compare the simulated ENSO activity with the proxy and other experiments, the marine sediment off Peru and the number of El Niño events simulated by the ZC model, which were obtained from Clement et al. (1999) (hereafter C99), are shown in Figure 3b together with our Tran-ZC run. In C99, the deviation of solar forcing with respect to the present was simply added to the SST equation as diabatic heating. Interestingly, as seen in Figure 3b, the observed proxy data somewhat well matched the C99 results, especially after 4,000 years B.P., while around 6,000 years B.P., a large number of ENSO events in C99 and a low number of events until ~5,000 years B.P. are shown, which did not match the proxy data. On the other hand, our experiment matched the proxy data rather well, such as suppressed ENSO activity between 6,000 and 5,500 years B.P. and an abrupt enhancement of ENSO activity around 5,500 years B.P. However, a slight suppression of ENSO activity between 1,000 and 500 years B.P. that appeared in the proxy data was not well simulated by our experiment.

A perfect match between the model simulation and observation could not be expected, but overall, our simulation followed the observations well. Therefore, we can conclude that the mean state, including SST, thermocline depth, ocean stratification, and surface wind stress, modified by orbital forcing led to changes in ENSO activity during the last 6,000 years.

In order to ascertain which background state was most influential on modulating ENSO activity over time, we performed a sensitivity experiment in which a background state was varied over time while the others were fixed at their present ones (i.e., 0 ka). The implemented background states were as follows: mean SST ("SST_m experiment"), mean thermocline ("H_m experiment"), mean stratification (i.e., vertical temperature gradient; $\frac{d\overline{T}}{dz}$) ("$dTdz_m$ experiment"), and mean wind stress ("WS_m experiment"). We performed 51 runs for each sensitivity experiment, and then the ensemble mean was taken. All of the results are presented as 101 year moving STDs of the Niño-3 SST anomalies. As shown in Figure 3c, the SST_m experiment showed that the suppressed ENSO variability at 6,000 years B.P. gradually increased over time, but the ENSO variability was relatively stronger compared to Tran-ZC run. The H_m experiment also showed a gradual enhancement of ENSO activity, but its variability was wider than that of the SST_m experiment. Both the $dTdz_m$ and WS_m experiments showed strong ENSO activity over time, like the 0 ka-ZC run. Although none of the sensitivity experiments were significantly correlated with the control experiment (as seen in Figure 3c), the SST_m experiment most closely resembled the control experiment. Note that in order to figure out the impact of annual cycle change, we further performed a sensitivity experiment, in which the annual cycle of climatological mean SST without annual mean

was varied through ZC model run, while others were fixed at their present ones. The result did not show any significant trend in ENSO amplitude (not shown here). Therefore, our experiment suggested that the slowly varying annual mean is more important than annual cycle part in changing of ENSO amplitude during the last 6,000 years.

Finally, we computed the regression of each background state with respect to the 101 year moving STD of the Niño-3 SST anomalies (Figure 4). The background states were obtained from LOVECLIM experiments, where the last 100 year mean of the background state was removed, and the Niño-3 SST anomalies were chosen from one ensemble of Tran-ZC run, which is very similar to the ensemble-mean. These regressions indicate the background states related to the change in ENSO activity during the last 6,000 years. As expected, each regression map is well matched to each prescribed background state. In other words, Figure 4 is like a mirror image of Figure 2. Therefore, the background-state change in Figure 2 should be considered as a main factor in modifying ENSO activity during the last 6,000 years.

4. Summary and Possible Explanation

Using LOVECLIM, we performed a transient simulation for the last 6,000 years in which only orbital forcing was updated over time. To investigate the impact of background state changes on ENSO variability, slowly varying background states obtained from LOVECLIM were applied to the intermediate air-sea coupled model for ENSO (the ZC model). ENSO variability simulated by the ZC model resembled the observed ENSO variability obtained from paleo-proxy data quite closely, indicating that the slowly varying of climate background state during the last 6,000 years associated with changes in orbital forcing solely was able to modify ENSO variability similar to that observed. From sensitivity experiments with the ZC model on each background climate state, we found that one background state only experiment was not able to fully rule out the Tran-ZC run, so the combined effect of various background states was important. Nevertheless, we propose that at least under the ZC model framework, changes in the horizontal advections associated with changes in the horizontal gradient of the mean SST may be critical in modifying ENSO activity for the last 6,000 years. The explanation of this is as follows.

Following the formula of the ZC model, we can estimate the possible contribution of each process either qualitatively or quantitatively. The following estimation in % represents not the amplitude change of ENSO but a feedback strength involved in each process.

1. Mean SST gradient: Enhanced both zonal and meridional gradient of the mean SST (An & Choi, 2014; see Figure 2a) over the EP during the 6,000 years B.P. influenced ENSO activity through the mean SST advection by anomalous zonal current ($-u\frac{\partial \overline{T}}{\partial x}$) and meridional current ($-v\frac{\partial \overline{T}}{\partial y}$) (e.g., An et al., 2004).
2. Mean SST: Cool SST (about −0.2°C colder over equatorial Pacific; Figure 2a) during the MH suppressed atmospheric convection in response to SST anomalies, and so reduced ENSO activity (Liu et al., 2000). From the atmospheric heating formula in the ZC model, $Q = (\text{const}*T)\exp\left[(\overline{T} - 30^{\circ}\text{C})/16.7^{\circ}\text{C}\right]$, where T and $\overline{T}$ are anomaly and mean, respectively, and 1.2% of the reduction of the atmospheric heating rate during 6,000 years ago compared to the present was estimated, indicating a weak contributor.
3. Mean thermocline depth: By differentiating the T_{sub} formula with respect to h (A13 of Zebiak and Cane (1987)), the rate of subsurface temperature change against thermocline depth change becomes

$$\frac{\partial T_{sub}}{\partial h} = \begin{cases} T_1 b_1 \,\text{sech}^2\left[b_1(\overline{h}+h)\right] & \text{for } h > 0 \\ -T_2 b_2 \,\text{sech}^2\left[b_2(\overline{h}-h)\right] & \text{for } h < 0 \end{cases} \quad (3)$$

where T_1 = 28°C, T_2 = −40°C, $b_1 = (80\text{ m})^{-1}$, and $b_2 = (33\text{ m})^{-1}$ (A13 in Zebiak and Cane (1987)). Therefore, $\frac{\partial T_{sub}}{\partial h}$ for 6,000 years B.P. ($\overline{h}$ = 52 m; Figure 2c) was reduced by about 3.2% compared to the present ($\overline{h}$ = 50 m; Zebiak & Cane, 1987) for h = 10 m. Similarly, for h = − 10 m, the reduction was about 10.9%. Therefore, the reduction of ENSO during 6,000 years B.P. by the deepening of H_m is understandable.
4. Mean vertical temperature gradient: The mean vertical temperature gradient in the original ZC model was about 5°C $(100\text{ m})^{-1}$ over the EP, while its difference between 6,000 years B.P. and the present (Figure 2d) was about −0.1°C $(100\text{ m})^{-1}$. Therefore, a 2% reduction was expected.

5. Mean winds: Mean winds modify the convergence feedback in the atmospheric heating term, i.e., $Q_c = \text{const}*[M(\overline{c}+c) - M(\overline{c})]$, where c is the surface wind convergence and $M(x) = x$, for $x > 0$; otherwise, $M(x) = 0$. Therefore, if there was no change of sign in the mean convergence, as inferred from Figure 2b, the influence of mean wind change might have been tiny (i.e., Figure 3c).

This discussion may provide some insights into which background state was more influential in modifying ENSO activity during the last 6,000 years. However, implementing only one background state in the ZC model (i.e., dynamically imbalanced states) could still have resulted in rather unrealistic ENSO variability. Therefore, the sensitivity experiments should be interpreted with caution, although at the very least, the importance on the combined effects of the background states on modifying ENSO activity over time was clearly addressed.

Acknowledgments
This research was supported by Basic Science Research Program through the National Research Foundation of Korea (NRF) (NRF-2017R1A2A2A05069383). Model output are available at http://web.yonsei.ac.kr/climatelab/Data.htm.

References

An, S.-I., & Bong, H. (2016). Inter-decadal change in El Niño–Southern Oscillation examined with Bjerknes stability index analysis. *Climate Dynamics*, *47*(3-4), 967–979. https://doi.org/10.1007/s00382-015-2883-8

An, S.-I., & Bong, H. (2018). Feedback process responsible for the suppression of ENSO activity during the mid-Holocene. *Theoretical and Applied Climatology*. https://doi.org/10.1007/s00704-017-2117-6

An, S.-I., & Choi, J. (2014). Mid-Holocene tropical pacific climate state, annual cycle, and ENSO in PMIP2 and PMIP3. *Climate Dynamics*, *43*(3–4), 957–970. https://doi.org/10.1007/s00382-013-1880-z

An, S.-I., & Choi, J. (2015). Why the twenty-first century tropical pacific trend pattern cannot significantly influence ENSO amplitude? *Climate Dynamics*, *44*(1–2), 133–146. https://doi.org/10.1007/s00382-014-2233-2

An, S.-I., & Jin, F.-F. (2000). An Eigen analysis of the interdecadal changes in the structure and frequency of ENSO mode. *Geophysical Research Letters*, *27*(16), 2573–2576. https://doi.org/10.1029/1999GL011090

An, S.-I., Timmermann, A., Bejarano, L., Jin, F.-F., Justino, F., Liu, Z., & Tudhope, A. W. (2004). Modeling evidence for enhanced El Niño–Southern Oscillation amplitude during the Last Glacial Maximum. *Paleoceanography*, *19*, PA4009. https://doi.org/10.1029/2004PA001020

An, S.-I., & Wang, B. (2000). Interdecadal change of the structure of the ENSO mode and it impact on the ENSO frequency. *Journal of Climate*, *13*(12), 2044–2055. https://doi.org/10.1175/1520-0442(2000)013%3C2044:ICOTSO%3E2.0.CO;2

Bjerknes, J. (1966). A possible response of the atmospheric Hadley circulation to equatorial anomalies of ocean temperature. *Tellus*, *18*, 820–829.

Brovkin, V., Ganapolski, A., & Svirezhev, Y. (1997). A continuous climate-vegetation classification for use in climate-biosphere studies. *Ecological Modelling*, *101*, 251–261.

Cane, M. A., & Zebiak, S. E. (1987). Prediction of E1 Niño events using a physical model. In H. Cattel (Ed.), *Atmosphere and ocean variability* (pp. 153–182). Reading, UK: Royal Meteorological Society Press.

Chen, D., Cane, M. A., Zebiak, S. E., & Kaplan, A. (1998). The impact of sea level data assimilation on the Lamont model prediction of the 1997/1998 E1 Niño. *Geophysical Research Letters*, *25*(15), 2837–2840. https://doi.org/10.1029/98GL52186

Clement, A. C., Seager, R., & Cane, M. A. (1999). Orbital controls on the El Niño/Southern Oscillation and the tropical climate. *Paleoceanography*, *14*, 441–456.

Clement, A., Seager, R., & Cane, M. (2000). Suppression of El Niño during the mid-Holocene by changes in the Earth's orbit. *Paleoceanography*, *15*(6), 731–737. https://doi.org/10.1029/1999PA000466

Conroy, J. L., Overpeck, J. T., Cole, J. E., Shanahan, T. M., & Steinitz-Kannan, M. (2008). Holocene changes in eastern tropical Pacific climate inferred from a Galapagos lake sediment record. *Quaternary Science Reviews*, *27*(11-12), 1166–1180. https://doi.org/10.1016/j.quascirev.2008.02.015

Fedorov, A. V., & Philander, S. G. (2001). A stability analysis of tropical ocean-atmosphere interactions: Bridging measurements and theory for El Niño. *Journal of Climate*, *14*(14), 3086–3101. https://doi.org/10.1175/1520-0442(2001)014%3C3086:ASAOTO%3E2.0.CO;2

Flügel, M., & Chang, P. (1999). Stochastically induced climate shift of El Niño–Southern Oscillation. *Geophysical Research Letters*, *26*(16), 2473–2476. https://doi.org/10.1029/1999GL900550

Flügel, M., Chang, P., & Penland, C. (2004). The role of stochastic forcing in modulating ENSO predictability. *Journal of Climate*, *17*(16), 3125–3140. https://doi.org/10.1175/1520-0442(2004)017%3C3125:TROSFI%3E2.0.CO;2

Gill, A. E. (1980). Some simple solutions for heat-induced tropical circulation. *Quarterly Journal of the Royal Meteorological Society*, *106*(449), 447–462. https://doi.org/10.1002/qj.49710644905

Goosse, H., & Fichefet, T. (1999). Importance of ice-ocean interactions for the global ocean circulation: a model study. *Journal of Geophysical Research*, *104*(C10), 23,337–23,355.

Goosse, H., Brovkin, V., Fichefet, T., Haarsma, R., Jongma, J., Huybrechts, P., et al. (2010). Description of the Earth system model of intermediate complexity LOVECLIM version 1.2. *Geoscientific Model Development*, *3*, 603–633.

Huybrechts, P. (2002). Sea-level changes at the LGM from ice-dynamic reconstructions of the Greenland and Antarctic ice sheets during the glacial cycles. *Quaternary Science Review*, *21*, 203–231.

Jin, F.-F., Lin, L., Timmermann, A., & Zhao, J. (2007). Ensemble-mean dynamics of the ENSO recharge oscillator under state-dependent stochastic forcing. *Geophysical Research Letters*, *34*, L03807. https://doi.org/10.1029/2006GL027372

Jin, F.-F., Neelin, J. D., & Ghil, M. (1994). El Niño on the Devil's Staircase: Annual and Subharmonic Steps to Chaos. *Science*, *264*, 70–72.

Karamperidou, C., DiNezio, P. N., Timmermann, A., Jin, F.-F., & Cobb, K. M. (2015). The response of ENSO flavors to mid-Holocene climate: Implications for proxy interpretation. *Paleoceanography*, *30*, 527–547. https://doi.org/10.1002/2014PA002742

Koutavas, A., & Joanides, S. (2012). El Niño–Southern Oscillation extrema in the Holocene and Last Glacial Maximum. *Paleoceanography*, *27*, PA4208. https://doi.org/10.1029/2012PA002378

Liu, Z., Kutzbach, J., & Wu, L. (2000). Modeling climate shift of El Niño variability in the Holocene. *Geophysical Research Letters*, *27*(15), 2265–2268. https://doi.org/10.1029/2000GL011452

Liu, Z., Lu, Z., Wen, X., Otto-Bliesner, B. L., Timmermann, A., & Cobb, K. M. (2014). Evolution and forcing mechanisms of El Niño over the past 21,000 years. *Nature*, *515*(7528), 550–553. https://doi.org/10.1038/nature13963

McGregor, H. V., & Gagan, M. K. (2004). Western Pacific coral δ18O records of anomalous Holocene variability in the El Niño-Southern Oscillation. *Geophysical Research Letters*, *31*, L11204. https://doi.org/10.1029/2004GL019972

McPhaden, M. J., Zebiak, S. E., & Glantz, M. J. (2006). ENSO as an integrating concept in Earth science. *Science*, *314*(5806), 1740–1745. https://doi.org/10.1126/science.1132588

Mouchet, A., & François, L. M. (1996). Sensitivity of a global oceanic carbon cycle model to the circulation and to the fate of organic matter: preliminary results. *Physics and Chemistry of the Earth*, *21*(5–6), 511–516.

Moy, C. M., Seltzer, G. O., Rodbell, D. T., & Anderson, D. M. (2002). Variability of El Niño/Southern Oscillation activity at millennial timescales during the Holocene epoch. *Nature*, *420*(6912), 162–165. https://doi.org/10.1038/nature01194

Opsteegh, J. D., Haarsma, R. J., Selten, F. M., & Kattenberg, A. (1998). ECBILT: A dynamic alternative to mixed boundary conditions in ocean models. *Tellus*, *50A*, 348–367.

Rein, B., Lückge, A., Reinhardt, L., Sirocko, F., Wolf, A., & Dullo, W.-C. (2005). El Niño variability off Peru during the last 20,000 years. *Paleoceanography*, *20*, PA4003. https://doi.org/10.1029/2004PA001099

Rein, B., Lückge, A., & Sirocko, F. (2004). A major ENSO anomaly during the Medieval period. *Geophysical Research Letters*, *31*, L17211. https://doi.org/10.1029/2004GL020161

Thompson, C. J., & Battisti, D. S. (2001). A linear stochastic dynamical model of ENSO. Part II: Analysis. *Journal of Climate*, *14*(4), 445–466. https://doi.org/10.1175/1520-0442(2001)014%3C0445:ALSDMO%3E2.0.CO;2

Timmermann, A., Jin, F.-F., & Abshagen, J. (2003). A nonlinear theory for El Niño bursting. *Journal of the Atmospheric Sciences*, *60*(1), 152–165. https://doi.org/10.1175/1520-0469(2003)060%3C0152:ANTFEN%3E2.0.CO;2

Tudhope, A. W., Chilcott, C. P., McCulloch, M. T., Cook, E. R., Chappell, J., Ellam, R. M., et al. (2001). Variability in the El Niño–Southern Oscillation through a glacial-interglacial cycle. *Science*, *291*(5508), 1511–1517. https://doi.org/10.1126/science.1057969

Wang, B., & An, S.-I. (2001). Why the properties of El Niño changed during the late 1970s. *Geophysical Research Letters*, *28*(19), 3709–3712. https://doi.org/10.1029/2001GL012862

Wanner, H., Beer, J., Bütikofer, J., Crowley, T. J., Cubasch, U., Flückiger, J., et al. (2008). Mid- to late Holocene climate change: An overview. *Quaternary Science Reviews*, *27*(19-20), 1791–1828. https://doi.org/10.1016/j.quascirev.2008.06.013

Yeh, S.-W., & Kirtman, B. P. (2004). Tropical Pacific decadal variability and ENSO amplitude modulation in a CGCM. *Journal of Geophysical Research*, *109*, C11009. https://doi.org/10.1029/2004JC002442

Yeh, S.-W., Kug, J.-S., & An, S.-I. (2014). Recent progress on two types of El Niño: Observation, dynamics, and future changes. *Asia-Pacific Journal of Atmospheric Sciences*, *50*(1), 69–81. https://doi.org/10.1007/s13143-014-0028-3

Zebiak, S. E., & Cane, M. A. (1987). A model El Niño-Southern Oscillation. *Monthly Weather Review*, *115*, 2262–2278.